

December 7, 2006  
Prepared for *J. Phys. Chem.*

## **Adaptive Partitioning in Combined Quantum Mechanical and Molecular Mechanical Calculations of Potential Energy Functions for Multiscale Simulations**

**Andreas Heyden<sup>\*‡</sup>, Hai Lin<sup>†</sup>, and Donald G. Truhlar<sup>\*‡</sup>**

*Department of Chemistry and Supercomputing Institute, University of Minnesota, Minneapolis, Minnesota 55455-0431 and Department of Chemistry, University of Colorado at Denver and Health Science Center, Denver, Colorado 80217-3364*

In many applications of multilevel/multiscale methods, an active zone must be modeled by a high-level electronic structure method, while a larger environmental zone can be safely modeled by a lower-level electronic structure method, molecular mechanics, or an analytic potential energy function. In some cases though, the active zone must be redefined as a function of simulation time. Examples include a reactive moiety diffusing through a liquid or solid, a dislocation propagating through a material, or solvent molecules in a second coordination sphere (which is environmental) exchanging with solvent molecules in an active first coordination shell. In this article, we present a procedure for combining the levels smoothly and efficiently in such systems in which atoms or groups of atoms move between high-level and low-level zones. The method dynamically partitions the system into the high-level and low-level zones and, unlike previous algorithms, removes all discontinuities in the potential energy and force whenever atoms or groups of atoms cross boundaries and change zones. The new adaptive partitioning (AP) method is compared to Rode's "hot spot" method and Morokuma's "ONIOM-XS" method that were designed for multilevel MD simulations. MD simulations in the microcanonical ensemble show that the AP method conserves both total energy and momentum, while the ONIOM-XS method fails to conserve total energy,

and the hot spot method fails to conserve both total energy and momentum. Two versions of the AP method are presented, one scaling as  $O(2^N)$  and one with linear scaling in  $N$ , where  $N$  is the number of groups in a buffer zone separating the active high-level zone from the environmental low-level zone. The AP method is also extended to systems with multiple high-level zones to allow, e.g., the study of ions and counterions in solution using the multilevel approach.

\*Corresponding authors. Email: heyden@chem.umn.edu; truhlar@umn.edu.

‡ University of Minnesota

† University of Colorado

## 1. Introduction

Increasing computational resources and improved algorithms are stimulating more realistic simulations of condensed-phase processes and complex materials at the atomic level and thereby motivating the development of more flexible and more efficient algorithms. Methods for modeling potential energy functions that are commonly employed for the study of large systems, for example molecular mechanics,<sup>1</sup> analytic potential energy functions,<sup>2,3</sup> or affordable direct dynamics methods,<sup>4</sup> are often not accurate enough to describe the atomistic dynamics at active sites where solute-solvent coupling is strong and dynamic, where dislocations or cracks are forming, where grain boundaries are moving, or where reaction is occurring. In contrast, high-level electronic structure methods that model these features accurately are too computationally expensive to be used for long-time simulations, large systems, or full ensemble averaging. One solution is to use multilevel methods such as combined QM/MM methods that combine

quantum mechanical (QM) electronic structure for an active zone with molecular mechanics (MM) for an environmental zone.<sup>5-24</sup> (By MM, we mean any generally parameterized analytic potential.) The efficiency of such multilevel methods allows one to perform accurate calculations for large and complex systems over long time scales. Although we use the language of QM and MM, the method is equally applicable to combining high-level QM with low-level MM or combining high-level MM (e.g., a many-body potential) with low-level MM (e.g., a pairwise additive potential).

Most systems studied with multilevel methods that are based on partitioning consist of a small localized active region treated at a high level of theory (the active zone) immersed in an extended system treated at a low level of theory (the environmental zone). To study the dynamical and structural properties of these systems, the multilevel methods are combined with sampling schemes and/or dynamical methods, such as molecular dynamics (MD) or Monte Carlo (MC) algorithms. When the active region in these systems is localized, the same atoms are in the active region during the entire simulation, and the level of theory used to describe their interaction does not change during the simulation.

In the present article, we are interested in systems with non-localized active regions, such as processes in solution,<sup>25-30</sup> diffusion, reaction, and island evolution studies on catalytic surfaces or nanoparticles or in membranes,<sup>31-35</sup> defect propagation in materials,<sup>36</sup> and complex gas-phase reactive systems.<sup>37</sup> The method presented here can be used to combine multilevel methods with sampling schemes for systems with atoms or groups of atoms entering or leaving the active zone (the QM region) during the simulation. Since an atom should be treated at a high level of theory when it is in the

active zone (for accuracy) and at a lower level of theory otherwise (for efficiency) the level of theory used to describe an atom changing zones changes during the simulation. A simple change in the level of theory used to describe the interaction of an atom with the surrounding atomistic environment would result in a discontinuity in the potential energy and force on each atom in the system. Since the quality of the level of theories used to describe the atoms in the system often differs significantly, the discontinuities in the potential energy and forces can be large and can result in numerical instabilities,<sup>38</sup> a lack of conservation of total energy in a molecular dynamics simulation, sampling of configuration space from an unknown, possibly non-equilibrium ensemble,<sup>39</sup> and simulation results that show artifacts.<sup>40</sup>

The algorithm presented here removes all discontinuities in the potential energy and force whenever atoms or groups of atoms cross zone boundaries. Two versions of the new method are presented, one scaling as  $O(2^N)$  and one with linear scaling in  $N$ , where  $N$  is the number of groups in a buffer zone.

The article is organized as follows. In Section 2, previous methods developed for combining multilevel methods with sampling schemes are reviewed and their strengths and weaknesses are analyzed. Section 3 introduces a new method for dynamically partitioning a multilevel system into high-level and low-level zones such that all discontinuities are removed in the potential energy and force whenever atoms or groups of atoms change zones. Applications of two versions of the newly developed method are presented in section 4, and the results are compared to those obtained by the “hot spot” method of Rode<sup>41,42</sup> and the ONIOM-XS method of Kerdcharoen and Morokuma.<sup>39</sup> Although the active zone in these sample applications is a spherical region surrounding a

central atom, more generally the active zone may also be a molecular reagent or a complex, the active site of an enzyme, or any subsystem which one wants to treat at a high-level. In Section 5, extensions of the newly developed method are presented to simulate systems with multiple active regions that possibly merge during the simulation.

## 2. Previous adaptive multilevel methods

Rode and coworkers<sup>41-43</sup> were the first to study systems with a non-localized active region by MD simulations employing QM/MM potentials. In particular they studied the structure and dynamics of metal ions in solution.<sup>26,30,40</sup> To study the ligand exchange around a metal ion, they divided a system consisting of one metal ion and a few hundred solvent molecules into a spherical, high-level, active zone with radius  $r_{\min}$ , a small buffer zone surrounding the active zone, and the remainder of the system, which we will call the environmental zone.

In discussing Rode's hot spot algorithm, Kerdcharoen and Morokuma's ONIOM-XS algorithm, and our own adaptive partitioning algorithm, we will use the language of groups. A group may be an atom (e.g., a Ne atom for modeling solvation in a rare-gas liquid or for modeling a solid Ne host lattice), a molecule (for example a water molecule in aqueous solution), a protein residue, a monomer in a polymer, a formula unit in a solid salt, and so forth. At any time, all the atoms of a given group are always considered to be in the same zone. Although the schemes can all be defined more generally we will discuss them here in terms of a spherical active zone surrounded by a spherical-shell buffer zone, and an environmental zone (which comprises the rest of the system, which need not be spherical). The buffer zone was defined by Rode and coworkers as a shell

with inner and outer radii,  $r_{\min}$  and  $r_{\max}$ . The metal ion defines the center of the active zone in these ligand exchange studies, but more generally any one group, to be called the primary group, can be singled out, and the radial distance  $r$  is measured from that primary group. In practice, Rode chose the radius of the active zone such that the active zone includes the first<sup>26,42-67</sup> and sometimes also the second<sup>68-74</sup> solvation shell. The purpose of the buffer zone is to smooth the force components on groups, such as a water molecule, that are entering or leaving the active zone. The thickness of the buffer depends on the levels of theory used for the multilevel simulation and is usually chosen to be  $0.2 \text{ \AA}$ .<sup>41,42</sup> Figure 1 illustrates the partitioning of the system into multiple zones.

The potential energy,  $V$ , and the force,  $\mathbf{f}_i$ , acting on each atom,  $i$ , during the MD simulation are defined in Rode's hot spot method<sup>41,42</sup> in a similar way to the Integrated Molecular Orbital Molecular Mechanics (IMOMM) scheme of Maseras and Morokuma:<sup>7</sup>

$$V = V^{entire}(MM) + \left( V^{A+B}(QM) - V^{A+B}(MM) \right) \quad (1)$$

$$\mathbf{f}_i = \mathbf{f}_i^{entire}(MM) + S(r_i) \left( \mathbf{f}_i^{A+B}(QM) - \mathbf{f}_i^{A+B}(MM) \right) \quad (2)$$

where  $V^{entire}(MM)$  is the potential energy of the entire system calculated at the low level of theory, and  $V^{A+B}(QM)$  and  $V^{A+B}(MM)$  are the potential energies of all groups in the active (A) and buffer (B) zones treated at the high and low level of theory, respectively. The zero of energy is defined for both levels of theory as the sum of energies of the isolated groups, with each isolated group, in its equilibrium geometry (if it has more than one atom). The force components obtained from the gradients of the corresponding energy terms are  $\mathbf{f}_i^{entire}(MM)$ ,  $\mathbf{f}_i^{A+B}(QM)$ , and  $\mathbf{f}_i^{A+B}(MM)$ , each of

which is a 3-dimensional vector. To calculate trajectories in a MD simulation it is not necessary to determine the potential energy; only the forces need to be calculated, and Rode smoothed the force components of atoms belonging to groups in the buffer zone; this was accomplished by using the smoothing function  $S(r_i)$ :<sup>41</sup>

$$S(r_i) = \begin{cases} 1, & \text{for } r_i \leq r_{\min} \\ \frac{(r_{\max}^2 - r_i^2)^2 (r_{\max}^2 + 2r_i^2 - 3r_{\min}^2)}{(r_{\max}^2 - r_{\min}^2)^3}, & \text{for } r_{\min} < r_i < r_{\max} \\ 0, & \text{for } r_i \geq r_{\max} \end{cases} \quad (3)$$

where  $r_i$  is the radial coordinate of group  $i$ . In most applications of the hot spot method the potential energy is not evaluated or defined.<sup>41,44-77</sup>

An advantage of the hot spot method is that it does not need any additional high-level force calculations to determine the forces acting on atoms in the buffer zone. The hot spot method was criticized by Kerdcharoen and Morokuma because it employs a smoothing function only on groups in the buffer zone and therefore does not remove discontinuities in the force on atoms outside the buffer zone.<sup>38,39</sup> As a result, hot spot simulations suffer from numerical instabilities and do not conserve energy in MD simulations in the microcanonical ensemble. Furthermore, there is no potential energy expression corresponding to the forces so that the hot spot method cannot be applied to Monte Carlo or free energy simulations. Finally, momentum is not conserved in simulations using the hot spot method. Newton's third law is not fulfilled because only forces on atoms in the buffer zone are smoothed.

Rode and coworkers performed simulations in the canonical ensemble (called the *NVT* ensemble) using the Berendsen algorithm.<sup>78</sup> As a result, despite the lack of momentum conservation, the kinetic energy of the system is approximately constant, and

numerical instabilities are reduced. Nevertheless, not conserving energy and momentum in the conservative dynamics risks sampling of configuration space from an unknown, possibly non-equilibrium ensemble. For example, Kerdcharoen and Morokuma showed that a simple multilevel simulation scheme without the removal of discontinuities was not able to sample equilibrium configurations in *NVT* simulations.<sup>39</sup>

To remove some of the limitations of the hot spot method, Kerdcharoen and Morokuma<sup>39</sup> developed the ONIOM-XS (XS = eXtension to Solvation) method. In the ONIOM-XS method two multilevel energy calculations are performed whenever at least one group is present in the buffer zone. The smoothed potential energy is defined as:

$$V = PV^{A+B} + (1-P)V^A \quad (4)$$

where  $V^{A+B}$  is the potential energy determined with all groups in the active and buffer zone treated at the high level of theory, and  $V^A$  is the corresponding potential energy determined with only the active zone treated at the high level of theory. The smoothing function  $P$  is defined as the arithmetic average of the set of smoothing functions  $P_i(\alpha_i)$  for every individual group in the buffer zone:

$$P = \frac{1}{N} \sum_{i=1}^N P_i(\alpha_i) \quad (5)$$

where  $N$  is the number of groups in the buffer zone,  $P_i$  is a fifth order spline:

$$P_i(\alpha_i) = -6\alpha_i^5 + 15\alpha_i^4 - 10\alpha_i^3 + 1 \quad (6)$$

and  $\alpha_i$  is given by:

$$\alpha_i = \frac{r_i - r_{\min}}{r_{\max} - r_{\min}}, \quad \text{for} \quad r_{\min} < r_i < r_{\max} \quad (7)$$

The ONIOM-XS method removes all discontinuities in the potential energy and force if only one group is present in the buffer zone, but it fails to remove all discontinuities in the potential energy and force if more groups are present in the buffer zone ( $N$  changes discontinuously). As a result, the ONIOM-XS method does not conserve energy in an  $NVE$  simulation, and it is unclear whether equilibrium configurations are sampled in studies using the ONIOM-XS method in the general case.

### 3. The adaptive partitioning method

In this section, we present a simulation scheme that adaptively partitions a system into a high-level and a low-level zone in such a way that the composition of the high-level zone may change as a function of time (in MD) or as a function of the geometry of a sample (in MC). The scheme is designed to remove all discontinuities in the potential energy and forces whenever groups change zone. We call this method the adaptive partitioning method (AP). The method is equivalent to the ONIOM-XS method if only one group is present in the buffer zone and removes all discontinuities in the potential energy and force whenever more than one group is present.

#### 3.A. Permuted AP method

In one version of the AP method, called the permuted adaptive partitioning (permuted AP) method, the potential energy is defined as a linear combination of all possible combinations of multilevel energies that are obtained by treating the active zone and a subset of the  $N$  groups in the buffer zone at a high level of theory:

$$V = V \left( V^A, \left\{ V_i^A \right\}_{all}, \left\{ V_{i,j}^A \right\}_{all}, \dots, V_{1,2,\dots,N}^A \right) \quad (8)$$

where  $V^A$  is the energy determined with the active zone treated at the high level of theory.  $V_i^A$  is the energy determined with the active zone and group  $i$  in the buffer zone treated at the high level of theory.  $V_{i,j}^A$  is the energy determined with the active zone and groups  $i$  and  $j$  in the buffer zone treated at the high level of theory. Finally,  $V_{1,2,\dots,N}^A$  is the energy determined with the active and buffer zone treated at the high level of theory. For  $N$  groups in the buffer zone,  $2^N$  multilevel energy calculations are performed in the permuted AP method to obtain a smooth potential energy value.

The energy obtained by treating the active and buffer zone at the high level of theory can be written as:

$$\begin{aligned}
V_{1,2,\dots,N}^A = & V^A + \sum_{i=1,\dots,N} \left( V_i^A - V^A \right)_+ \\
& \sum_{\substack{i=1,\dots,N-1 \\ j=i+1,\dots,N}} \left( V_{i,j}^A - \left[ V^A + \sum_{r=i,j} \left( V_r^A - V^A \right) \right] \right)_+ \\
& \sum_{\substack{i=1,\dots,N-2 \\ j=i+1,\dots,N-1 \\ k=j+1,\dots,N}} \left( V_{i,j,k}^A - \left[ V^A + \sum_{r=i,j,k} \left( V_r^A - V^A \right) \right] \right)_+ \\
& \sum_{(p,q)=(i,j),(i,k),(j,k)} \left( V_{p,q}^A - \left[ V^A + \sum_{r=i,j} \left( V_r^A - V^A \right) \right] \right)_+ \\
& \dots
\end{aligned} \tag{9}$$

In the permuted AP method all high-level energy contributions from groups in the buffer zone are smoothed according to their radial coordinate:

$$\begin{aligned}
V = & V^A + \sum_{i=1, \dots, N} P_i (V_i^A - V^A)_+ \\
& \sum_{i=1, \dots, N-1} P_i P_j \left( V_{i,j}^A - \left[ V^A + \sum_{r=i,j} (V_r^A - V^A) \right] \right)_+ \\
& \sum_{i=1, \dots, N-2} P_i P_j P_k \left( V_{i,j,k}^A - \left[ V^A + \sum_{r=i,j,k} (V_r^A - V^A) \right] \right)_+ \\
& \sum_{j=i+1, \dots, N-1} P_i P_j P_k \left( V_{i,j,k}^A - \left[ V^A + \sum_{(p,q)=(i,j),(i,k),(j,k)} (V_{p,q}^A - V^A) \right] \right)_+ \\
& \dots
\end{aligned} \tag{10}$$

where  $P_i$  is a smoothing function. All derivatives of the potential energy with respect to the coordinates vary smoothly in this method up to the same order for which the smoothing functions  $P_i$  vary continuously. For example, if one uses the smoothing functions of equations 6 and 7, then  $V$  and its first and second derivatives are continuous.

In practical applications of the permuted AP method where the energy contribution of the terms in the series in equation 9 decrease rapidly, it may be advisable to truncate the series in equation 10. While this procedure significantly decreases the computational effort of the permuted AP method for systems with many groups in the buffer zone, it also creates small (but controllable) discontinuities in the potential energy and its derivatives.

### 3.B. Sorted AP method

While the permuted AP method can be used in multilevel MD and MC simulations, the computational effort of the permuted AP method scales poorly with the number of groups in the buffer zone. This section presents a method, the sorted adaptive partitioning (sorted AP) method, whose computational effort scales linearly with the

number of groups in the buffer zone. The modification requires that all groups in the buffer zone be sorted in some canonical order. We choose to sort the buffer-zone groups with respect to their radial coordinate, i.e., the buffer-zone group closest to the primary group is numbered 1, the next closest group is numbered 2, etc. Next,  $N + 1$  multilevel calculations are performed. One multilevel calculation has only the active zone treated at the high level of theory, one multilevel calculation has the active zone and group 1 in the buffer zone treated at the high level of theory, one multilevel calculation has the active zone and groups 1 and 2 in the buffer zone treated at the high level of theory, etc. The sorted AP potential  $V$  is a function of the  $N + 1$  computed multilevel energies, i.e.:

$$V = V\left(V^A, V_1^A, V_{1,2}^A, \dots, V_{1,2,\dots,N}^A\right) \quad (11)$$

Note that  $V_{1,2,\dots,j}^A$  is a multilevel calculation (in particular, a two-level calculation because the groups in the active zone and groups  $1, 2, \dots, j$  are treated at the high-level and all other groups in the buffer zone and in the environmental zone are treated at the low level). A smooth potential energy is computed in the sorted AP method by the recursion relation:

$$V_i = \Phi_i V_{1,2,\dots,i}^A + (1 - \Phi_i) V_{i-1}, \quad 1 \leq i \leq N \quad \text{with} \quad V_0 \equiv V^A \quad (12)$$

where  $\Phi_i$  is a smoothing function that depends on  $r_1, r_2, \dots, r_i$ , and  $V_N \equiv V$  is the potential energy of the system. The energy term,  $V_i$ , in equation 12 can be interpreted as a weighted sum of the energy  $V_{1,2,\dots,i}^A$  (calculated with the active zone and the first  $i$  groups in the buffer zone treated at the high level of theory) and an energy term  $V_{i-1}$

computed from weighted sums of energies that treat the active zone and up to  $i-1$  groups in the buffer zone at the high level of theory.

To compute the force on the atoms in the sorted AP method, equation 12 is rewritten as:

$$V = \sum_{i=0}^N \left( \Phi_i V_{1,2,\dots,i}^A \left[ \prod_{j=i+1}^N (1 - \Phi_j) \right] \right) \quad \text{with} \quad \Phi_0 \equiv 1 \quad (13)$$

For the sorted AP method to define a smooth potential energy (continuous first and second derivatives) the smoothing functions  $\Phi_j$  have to fulfill a number of requirements when group 1 crosses the boundary from  $r_1$  equals  $r_{\min} + \varepsilon \equiv r_{\min}^+$  to  $r_{\min} - \varepsilon \equiv r_{\min}^-$  (or when a group crosses in the opposite direction), when group  $N$  crosses the boundary from  $r_N$  equals  $r_{\max} - \varepsilon \equiv r_{\max}^-$  to  $r_{\max} + \varepsilon \equiv r_{\max}^+$ , or when groups  $m$  and  $l$  switch their order because  $r_l$  changes from  $r_m + \varepsilon \equiv r_m^+$  to  $r_m - \varepsilon \equiv r_m^-$ . (Note that we define  $\varepsilon$  as a positive infinitesimal.) We will summarize these requirements next. To simplify the notation, we will list only the arguments of  $\Phi_i$  that have critical values; thus, for example,  $\Phi_i(r_k = r_m^+)$  is shorthand for  $\Phi_i(r_1, r_2, \dots, r_k = r_m^+, \dots, r_i)$ . The continuity conditions at the inner boundary are

$$\Phi_1(r_1 = r_{\min}^+) = 1 \quad (14)$$

$$\Phi_j(r_1 = r_{\min}^+) = \Phi_{j-1}(r_1 = r_{\min}^-) \quad \text{for} \quad j = 2, \dots, N \quad (15)$$

$$\text{grad}(\Phi_1(r_1 = r_{\min}^+)) = \mathbf{0} \quad (16)$$

$$\text{grad}(\Phi_j(r_1 = r_{\min}^+)) = \text{grad}(\Phi_{j-1}(r_1 = r_{\min}^-)) \quad \text{for} \quad j = 2, \dots, N \quad (17)$$

those at the outer boundary are

$$\Phi_N \left( r_N = r_{\max}^- \right) = 0 \quad (18)$$

$$\Phi_j \left( r_N = r_{\max}^+ \right) = \Phi_j \left( r_N = r_{\max}^- \right) \quad \text{for } j = 1, \dots, N-1 \quad (19)$$

$$\text{grad} \left( \Phi_N \left( r_N = r_{\min}^+ \right) \right) = \mathbf{0} \quad (20)$$

$$\text{grad} \left( \Phi_j \left( r_N = r_{\min}^+ \right) \right) = \text{grad} \left( \Phi_j \left( r_N = r_{\min}^- \right) \right) \quad \text{for } j = 1, \dots, N-1 \quad (21)$$

and whenever the ordering of two groups  $m$  and  $m+1$  in the buffer zone changes, we require

$$\Phi_m \left( r_{m+1} = r_m^+ \right) = 0 \quad (22)$$

$$\text{grad} \left( \Phi_m \left( r_{m+1} = r_m^+ \right) \right) = \mathbf{0} \quad (23)$$

$$\text{grad} \left( \Phi_j \left( r_{m+1} = r_m^+ \right) \right) = \text{grad} \left( \Phi_j \left( r_{m+1} = r_m^- \right) \right) \quad \text{for } j = 1, \dots, N \quad (24)$$

Equations 14 - 24 make it clear why we defined the smoothing functions  $\Phi_j$  to depend on the coordinates of all groups in the buffer zone. (Smoothing function  $\Phi_j$  has to depend on group  $m-1$ ,  $m$ , and  $m+1$  to consider changes in the ordering of group  $m$ . In addition,  $\Phi_j$  has to depend on all other groups that might change ordering with group  $m-1$  and  $m+1$ . And so on, until it depends on all coordinates.)

One possible functional form for the smoothing functions,  $\Phi_i$ , is given by

$$\Phi_i = (1 + \chi_i)^{-3} \quad (25)$$

where

$$\chi_i = \sum_{j=1}^{i-1} \frac{1 - P_j}{P_j - P_i} + \frac{1 - P_i}{P_i} + \sum_{j=i+1}^N \frac{1 - P_i}{P_i - P_j} P_j \quad (26)$$

where  $P_i$  is a one-dimensional smoothing function; we will use the function given in equation 6. Figure 2 illustrates the variation of the smoothing functions  $\Phi_1$ ,  $\Phi_2$ , and  $\Phi_3$  for a system with three groups,  $i, j, k$ , in the buffer zone. Group  $i$  is moving through the buffer zone (initially group 1, then group 2, and finally group 3), group  $j$  is located at  $(r_j - r_{\min})/(r_{\max} - r_{\min}) = 0.1$ , and group  $k$  is located at  $(r_k - r_{\min})/(r_{\max} - r_{\min}) = 0.5$ . As required by equation 22, the smoothing functions  $\Phi_1$  and  $\Phi_2$  are zero when group  $i$  and  $j$  change their order, and  $\Phi_2$  and  $\Phi_3$  are zero when group  $i$  and  $k$  change their order.

There are many possible functional forms for the sorted smoothing functions,  $\Phi_i$ . Sometimes they must change rapidly to satisfy all the constraints, as shown in Figure 2. Under these circumstances, the force component from the gradient of the smoothing functions  $\Phi_1$  and  $\Phi_2$  can give a significant contribution to the force on the atoms in the buffer zone and the primary group in the active zone (to fulfill Newton's third law the gradient of  $\Phi_i$  exerts a force on these groups through the gradient of  $P_i$ ). In particular, the sign of the force from the gradient of the smoothing functions changes when the sort order changes. The magnitude of this force component depends on the functional form of the smoothing functions  $\Phi_i$ . The force components from the smoothing functions almost cancel if the levels of theory used to calculate the energy give similar results, e.g., if the energy differences between  $V^A$ ,  $V_1^A$ , and  $V_2^A$  are small.

To evaluate the quality of a number of functional forms for the smoothing functions  $\Phi_i$ , we performed multiple tests using the sorted AP method with different functional forms for the smoothing functions  $\Phi_i$ . Some of these tests are given in

supporting information. These tests show that the function in equation 25 is a reasonable choice, and we will use this choice in the rest of this article.

To conclude, the number of multilevel calculations required to define a smooth potential energy (whenever groups of atoms cross boundaries and change subsystem) is reduced in the sorted AP method in comparison to the permuted AP method by sorting the groups in the buffer zone and using “smart” smoothing functions that depend on the coordinates of all groups in the buffer zone.

## **4. Comparison of multilevel simulation schemes**

### **4.A. H<sub>2</sub>O molecule leaves the first solvation shell of a Li<sup>+</sup> ion**

In this section, we compare the two versions of the newly developed AP method with Rode’s hot spot method<sup>41,42</sup> and Kerdcharoen and Morokuma’s ONIOM-XS method<sup>39</sup> for the path of a water molecule leaving the first solvation shell of a Li<sup>+</sup> ion. Lithium salts are widely used in industrial applications, synthesis, and medicine, and they have been studied theoretically by San-Roman et al.,<sup>79</sup> Loeffler et al.,<sup>47,75,80</sup> and Spangberg et al.<sup>81</sup> Since the inclusion of many-body effects is often crucial for the description of ions in solution,<sup>81,82</sup> Loeffler et al.<sup>47,75,80</sup> studied the hydration of Li<sup>+</sup> by hot spot MD simulations with a QM/MM potential. We will use this system to illustrate the change in potential energy and force when a water molecule leaves the first solvation shell of a Li<sup>+</sup> ion, crosses the buffer zone, and enters the environmental zone in a simulation using the hot spot, ONIOM-XS, permuted AP, and sorted AP methods. The model system studied consists of one Li<sup>+</sup> ion (the primary group defining the center of the active zone) and eight water molecules. Initially, four water molecules (the first

solvation shell around the  $\text{Li}^+$  ion) are in the active zone with radius  $7 a_0$ , where  $1 a_0 \equiv 1 \text{ bohr} = 0.5292 \text{ \AA}$ , two water molecules are in a buffer zone that is  $1 a_0$  thick, and two water molecules are in the environmental zone. Figure 3 illustrates the initial configuration of the system of  $\text{Li}^+$  in water that was obtained by minimizing the potential energy from a random configuration of the system with the low-level potential used to describe the interaction between the molecules. The low-level intermolecular potential between the water molecules was computed with the CF2 water model<sup>83</sup> augmented with an intramolecular three-body potential (BJH water model).<sup>84</sup> The low-level  $\text{Li}^+ - \text{H}_2\text{O}$  interactions were described by a three-body potential from Loeffler and Rode.<sup>47,75,80,85</sup> For the high-level potential energy, we performed density functional calculations with the PBEh (also called PBE0) functional<sup>86,87</sup> with a very fine (m5)<sup>88</sup> numerical grid and a split valence basis set of double zeta quality with polarization functions (SV(P)).<sup>89</sup> The two levels are combined using the IMOMM scheme from Maseras and Morokuma.<sup>7</sup> The test consists of the movement of one water molecule from the first solvation shell of a cluster (we use a cluster rather than a liquid to provide a simple test case) into the environmental zone (see Figure 3). No other molecule is moved during the simulation. Each water molecule is a group. The distance of a water molecule to the primary group ( $\text{Li}^+$ ) is defined as the  $\text{Li}^+$ -to-O distance. Figure 4 illustrates the change of the potential energy along the path using the hot spot, ONIOM-XS, permuted AP, and sorted AP method. The potential energy varies smoothly in simulations using the permuted and sorted version of the AP method. In contrast, in simulations using the hot spot and ONIOM-XS method, there are significant discontinuities in the potential energy curve. In simulations using the hot spot method the discontinuity in the potential energy curve at the boundary

between buffer and environmental zone is 3 kcal/mol. In simulations using the ONIOM-XS method, there are two discontinuities in the potential energy curve on both sides of the boundary of the buffer zone of up to 1 kcal/mol. (The potential energy curves of the different methods do not agree in the active and environmental zone since at least two groups of atoms are always present in the buffer zone during the simulation, and all methods smooth their contributions differently.)

Figures 5 and 6 illustrate the change in the force (magnitude of atomic force vector) on atom H1, Li<sup>+</sup>, and O2 (see Figure 4) along the path. The variation of the force on atom H1, see Figure 5, is characteristic of most atoms in the system. Simulations with both versions of the newly developed AP method lead to smooth changes in forces whenever a group of atoms changes zones. Simulations with the hot spot and ONIOM-XS methods, in contrast, lead to significant jumps in the forces on the atoms in the system. Figure 6b illustrates that the only force components smoothed in the hot spot method are the ones from the moving group, i.e., the forces on atom O2. Furthermore, Figure 6 shows that the discontinuities in the forces in the ONIOM-XS simulation are often as large as in the hot spot method if multiple groups are present in the buffer zone. Finally, Figure 6a illustrates that there can be rapid non-monotonic changes in the force components in simulations using the sorted AP method. These rapid non-monotonic changes can occur if the energy difference between multilevel calculations computed with different groups treated at a high level of theory is significant. Rapid non-monotonic changes in the forces can be minimized by optimizing the low-level interaction potential for use in multilevel calculations with the high-level interaction

potential. No method joining low-level and high-level calculations will be free of such problems if the low-level method differs too greatly from the high-level one.

#### 4.B. *NVE* simulations

To analyze the consequences of discontinuities in the potential energy and its derivatives on molecular simulation results, we performed molecular dynamics simulations in the microcanonical ensemble (*NVE*). The model system consists of 171 argon atoms in a periodic box with a box length of 20 Å (this is a dense supercritical fluid for the conditions of our simulation).<sup>90</sup> One argon atom is chosen to be the primary group, and the radius of the active zone is  $r_{\min} = 5 \text{ \AA}$ . The interaction energy is calculated as the multilevel energy (IMMMM-type scheme)<sup>7</sup> with the Lennard-Jones potential

$$V_{ij} = 4 \varepsilon \left( \left( \frac{\sigma}{r_{ij}} \right)^{12} - \left( \frac{\sigma}{r_{ij}} \right)^6 \right) \quad (27)$$

describing the low-level interaction ( $\varepsilon = 0.23787 \text{ kcal/mol}$ ,  $\sigma = 3.405 \text{ \AA}$ )<sup>90</sup> and the Morse potential

$$V_{ij} = D \left[ 1 - e^{-a(r_{ij} - r_e)} \right]^2 - D \quad (28)$$

describing the high-level interaction ( $D = 0.23787 \text{ kcal/mol}$ ,  $r_e = 3.822 \text{ \AA}$ , and  $a = 1.570 \text{ \AA}^{-1}$ ). All pairwise interactions of argon atoms further than  $2.5\sigma$  apart were neglected. To remove the discontinuities in the low-level and high-level interaction potentials due to the cut-off radius, we used the shift-force modification of the Lennard-Jones and Morse potentials.<sup>91</sup> The initial configuration of the argon atoms in the *NVE*

simulations was obtained from a short *NVT* simulation at 180 K. Newton's equations of motion were integrated with the velocity Verlet algorithm<sup>92</sup> with a time step of 0.1 fs.

Figure 7 illustrates the total energy during the first 400 ps of simulations using the hot spot, ONIOM-XS, permuted AP, and sorted AP methods with a buffer zone 0.5 Å thick and also a scheme with an infinitesimally narrow buffer zone ( $r_{\min} = r_{\max} = 5.5 \text{ \AA}$ ). It is shown that both versions of the AP method conserve the total energy during the simulation. (Using a larger time step of 1 fs in simulations using the sorted AP method results in a small drift in the total energy of 0.02 kcal/mol.) Simulations using an infinitesimally narrow buffer zone or using the hot spot and the ONIOM-XS methods do not conserve total energy well; significant drifts in the total energy are observed, and they result in a continuous heating of the simulation system. Figure 8 illustrates the average temperature (averaged from the beginning of the simulation to time  $t$ ) of the simulation system. While the average temperature does not change in simulations using the AP method (it is about 172 K), the temperature increases to 195 K in simulations using the ONIOM-XS method. In simulations using an infinitesimally narrow buffer zone, the temperature increases to 202 K, and in simulations using the hot spot method the temperature increases to 319 K. It is interesting to note that simulations using the hot spot method heat up even faster than simulations using an infinitesimally narrow buffer zone, which is the same as no smoothing. In fact, the hot spot method caused the simulation to become unstable (total energy not conserved by many orders of magnitude) after 500 ps (not shown). In summary, the only simulation protocol that properly samples configurations from an equilibrium distribution is the AP method.

Figure 9a illustrates the radial distribution function (RDF) of the primary argon atom relative to all other argon atoms in the system. The RDFs are obtained from configurations sampled during the time interval from 200 to 1000 ps (due to stability problems in simulations using an infinitesimally narrow buffer zone and the hot spot method the sampling period is reduced in these simulations to the time interval from 200 to 400 ps). Figure 9a shows that the location of the buffer zone was chosen in all simulations to be between the first and second shell of argon atoms around the primary argon atom. The RDFs obtained with the permuted AP method and sorted AP method are essentially identical except for a small difference in the buffer zone. In contrast, simulations using an infinitesimally narrow buffer zone, the hot spot method, or the ONIOM-XS method lead to RDFs that differ significantly; the increase in the system temperature during the simulation leads to a reduction of all peaks in the RDF.

Figure 10a explains why simulations that use the hot spot method heat up even faster than those with an infinitesimally narrow buffer zone. The total momentum is not conserved in simulations using the hot spot method (unlike all other algorithms). The simulation system starts to drift in a random direction, and a convective flow of atoms is superimposed on the diffusive movement of the atoms.

To remove all discontinuities in the potential energy and force in multilevel simulations, the AP method performs multiple multilevel calculations per time step (in contrast to the hot spot method). During the MD simulations presented in this study the permuted version of the AP method performed on average 8.8 multilevel calculations per time step. The sorted AP method required 3.3 multilevel calculations per time step, and

the ONIOM-XS method needed 1.9 multilevel calculations per time step. On average 2.4 argon atoms were present in the buffer zone during the simulations.

#### **4.C. *NVT* simulations**

Since a number of studies have been published where ligand exchange rates and diffusion rates have been computed with the hot spot method in the *NVT* ensemble,<sup>29,42,61,62,64,66,67,74,76,77,80</sup> we repeated the argon simulations in the canonical ensemble to test the reliability of the computed data in these studies. The average temperature was set in these simulations at 172 K using the Nosé-Hoover two-chain thermostat.<sup>92</sup> Again the time step was 0.1 fs. Figure 9b illustrates the RDFs of the primary argon atom relative to all other argon atoms in the system. The RDFs are obtained from configurations sampled during the time interval from 200 to 1000 ps. All simulation protocols give similar RDFs with only small variations in the first peak height and around the buffer zone. Figure 10b illustrates the total momentum during the simulation in the *NVT* ensemble. Simulations using the hot spot method show a significant momentum drift and overall convective flow of argon atoms. As a result, we believe any dynamical property obtained with multilevel MD simulations using the hot spot method should be carefully analyzed.

#### **5. Extension to multiple active zones**

In this section, we extend the AP method to study systems with multiple active zones, including the possibility that they merge during the simulation. Examples of systems where this extension could be useful are solutions containing multiple ions and

counterions or a system of multiple reagents diffusing through a microporous catalyst. In the limit of only one active region the algorithm is equivalent to the one presented in section 3.

We assume that there are  $M$  active zones in the system that are each surrounded by a buffer zone. All active zones and their buffer zones are immersed in a single environmental zone. As before the buffer and environmental zones contain groups, and each active zone is centered on a primary group. Altogether there are  $N$  groups in the buffer zones. The first step of the AP method is to calculate the distance  $r_{ik}$  of all  $N$  groups  $i$  in the buffer zones to all  $M$  primary groups  $k$ . Notice that we have generalized  $r_i$  of previous sections to  $r_{ik}$ . Assuming spherical active zones, dimensionless distances are defined:

$$\alpha_{ik} = \frac{r_{ik} - r_{\min,k}}{r_{\max,k} - r_{\min,k}}, \quad \text{for} \quad r_{\min,k} < r_{ik} < r_{\max,k} \quad (29)$$

where  $r_{\min,k}$  and  $r_{\max,k}$  define the buffer zone around the active zone  $k$ . (The AP method is not limited to spherical active and buffer zones. In fact, both zones can have an arbitrary shape and only the parameter  $\alpha_{ik}$ , defined in equation 29, has to be adjusted to the geometric shape of both zones.) Next, the smoothing functions  $S_{ik}$  are calculated:

$$S_{ik} = -6\alpha_{ik}^5 + 15\alpha_{ik}^4 - 10\alpha_{ik}^3 + 1 \quad (30)$$

To define a global smoothing function  $P_i$  of group  $i$  in the system that is 0 only if all  $S_{ik}$  ( $k = 1, \dots, M$ ) are 0, 1 whenever at least one  $S_{ik}$  ( $k = 1, \dots, M$ ) is 1, and increases monotonously with increasing  $S_{ik}$  ( $k = 1, \dots, M$ ), we set:

$$P_i = 1 - \prod_{k=1}^M (1 - S_{ik}) \quad (31)$$

In the permuted AP method with multiple active zones, equation 10 is used where now  $V^A$  is the energy with only active zones treated at a high level of theory,  $V_i^A$  is the energy with active zones and group  $i$  in one of the buffer zones treated at a high level of theory, etc. Altogether,  $2^N$  calculations are performed in the permuted AP method to obtain a smooth potential energy and force whenever groups change subsystems or high-level active zones merge in the multilevel simulation.

For systems with one active zone, all groups in the buffer zone are sorted in the sorted AP method with respect to their  $P_i$  values, which measures their distance from the primary group (see section 3). For simulations with multiple active zones, all groups present in at least one buffer zone are sorted with respect to decreasing  $P_i$  values, although  $P_i$  is now more complex. In the sorted AP method with multiple active zones, the smoothing functions  $\Phi_i$  are again calculated using equation 25 and 26. The smooth potential energy is obtained in the sorted AP method using equation 13, where  $V_{1,2,\dots,i}^A$  is now the energy with the active zones and the first  $i$  groups in the buffer zones treated at a high level of theory. Altogether,  $N + 1$  multilevel calculations are performed in the sorted AP method for systems with multiple active zones.

## 6. Software

Quantum chemical electronic structure calculations have been performed with the TURBOMOLE V5.7 suite of programs.<sup>93</sup> The classical MD simulations presented in section 4 have been performed with the AP, ONIOM-XS, and hot spot algorithms added to the ANT program.<sup>94</sup> The permuted and sorted AP algorithms, for the cases of one or

multiple active zones, is being added as options to the QMMM package for combined quantum mechanical and molecular mechanical calculations.<sup>95</sup>

## 7. Conclusions

A new method, called the adaptive partitioning (AP) method, has been presented for combining multilevel methods, such as QM/MM methods, with sampling schemes, such as MD or MC methods, for applications to systems with non-localized active regions in which atoms or groups of atoms move between high-level and low-level zones. The method dynamically partitions the system into high-level and low-level zones and removes all discontinuities in the potential energy and force whenever groups of atoms cross boundaries and change zones. It has been demonstrated that multilevel MD simulations in the microcanonical ensemble that use the AP method conserve total energy and momentum. The AP method can be extended to study systems with multiple active zones that merge during the simulation, and therefore allows, e.g. the multilevel study of ions and counterions in solution or the study of molecules diffusing and reacting on catalytic surfaces and in membranes. Two versions of the new method have been presented, one scaling as  $O(2^N)$  and one with linear scaling in  $N$ , where  $N$  is the number of groups in one or more buffer zones separating the active zones from the environmental zone.

It has been shown that the hot spot and ONIOM-XS method, which are algorithms that were designed for multilevel MD simulations, do not remove all discontinuities in the potential energy and force on the atoms in the system. As a result, it is unclear if configurations from equilibrium distributions are sampled in simulations using these

algorithms.<sup>39</sup> The hot spot and ONIOM-XS methods did not conserve total energy in a multilevel MD test simulation of 171 argon atoms in a periodic box. The simulation system heated up significantly. The hot spot method also does not conserve momentum and performed worse in our test simulations than a method that does not alter the forces on the atoms at all when groups of atoms change subsystem; therefore, we do not recommend the hot spot method for demanding applications. The ONIOM-XS method performed in our tests slightly better than the hot spot method, but it only removes discontinuities in the potential energy and force if at most one group of atoms is present in the buffer zone. Under these circumstances, the algorithm is equivalent to the permuted AP method. Only when the ONIOM-XS method fails to compute a smooth potential energy and force does the AP method require more multilevel calculations. As a result, we believe the AP method should be used in multilevel simulations whenever the discontinuities in the potential energy and force are significant enough that equilibrium configurations cannot be sampled reliably with a simulation scheme that does not remove any discontinuities.

The tradeoff between the permuted and sorted version of the AP algorithm is as follows. The permuted AP scheme is more expensive but requires only mild continuity conditions on the permuted smoothing functions  $P_i$ . The sorted AP scheme is less expensive but places complicated constraints on the sorted smoothing functions  $\Phi_i$ . Nevertheless, these constraints are manageable, and the sorted AP is preferred for simulations of complex systems or systems with large active zones, where the average number of groups in the buffer zone may necessarily be large. If, however, the average number of groups in the buffer zone is only 2, the permuted AP is only about 33% more

expensive than the sorted AP, and it may be more efficient if it allows a larger time step because it yields a smoother potential energy function.

A key advantage of the way that we define the AP method is that it is blind to the choice of high-level and low-level methods. For example, the high-level theory could be coupled cluster theory and the low-level one could be Hartree-Fock theory, combined by an integrated molecular orbital method with a correlated capped subsystem,<sup>8</sup> or the high-level theory could be DFT, and the low-level one molecular mechanics, linked by generalized hybrid orbitals.<sup>19</sup>

**Acknowledgments:** The authors are grateful to Zhenhua Li for assistance. This work is supported in part by the Defense-University Research Initiative in Nanotechnology (DURINT) of the U. S. Army Research Laboratory and the U. S. Army Research Office under agreement number DAAD190110503 and by the office of Naval Research under award number N00014-05-1-0538. Computational resources were provided by the Minnesota Supercomputing Institute. A.H. gratefully acknowledges the Minnesota Supercomputing Institute for a research scholarship.

**Supporting Information Available:** Multiple test simulations using the sorted AP method with different functional forms for the smoothing functions  $\Phi_j$ . This material is available free of charge via the Internet at <http://pubs.acs.org>.

**References**

- (1) Bowen, J. P.; Allinger, N. L. *Rev. Comp. Chem.* **1991**, 2, 81.
- (2) Hill, J. R.; Sauer, J. *J. Phys. Chem.* **1995**, 99, 9536.
- (3) Lenosky, T. J.; Kress, J. D.; Kwon, I.; Voter, A. F.; Edwards, B.; Richards, D. F.; Yang, S.; Adams, J. B. *Phys. Rev. B* **1997**, 55, 1528.
- (4) Kim, Y.; Corchado, J. C.; Villa, J.; Xing, J.; Truhlar, D. G. *J. Chem. Phys.* **2000**, 112, 2718.
- (5) Singh, U. C.; Kollman, P. A. *J. Comput. Chem.* **1986**, 7, 718.
- (6) Field, M. J.; Bash, P. A.; Karplus, M. *J. Comput. Chem.* **1990**, 11, 700.
- (7) Maseras, F.; Morokuma, K. *J. Comput. Chem.* **1995**, 16, 1170.
- (8) Coitino, E. L.; Truhlar, D. G.; Morokuma, K. *Chem. Phys. Lett.* **1996**, 259, 159.
- (9) Eurenium, K. P.; Chatfield, D. C.; Brooks, B. R.; Hodoscek, M. *Int. J. Quantum Chem.* **1996**, 60, 1189.
- (10) *Combined Quantum Mechanical and Molecular Mechanical Methods*; Gao, J., Thompson, M. A., Eds.; ACS Symposium Series 712; American Chemical Society: Washington, DC, 1998.
- (11) Woo, T. K.; Cavallo, L.; Ziegler, T. *Theor. Chem. Acc.* **1998**, 100, 307.
- (12) Monard, G.; Merz, K. M. *Acc. Chem. Res.* **1999**, 32, 904.
- (13) Dapprich, S.; Komaromi, I.; Byun, K. S.; Morokuma, K.; Frisch, M. J. *J. Molec. Struct. (THEOCHEM)* **1999**, 462, 1.
- (14) Maseras, F. *Chem. Comm.* **2000**, 1821.
- (15) Sierka, M.; Sauer, J. *J. Chem. Phys.* **2000**, 112, 6983.

- (16) Gao, J. L.; Truhlar, D. G. *Annu. Rev. Phys. Chem.* **2002**, *53*, 467.
- (17) Sherwood, P.; de Vries, A. H.; Guest, M. F.; Schreckenbach, G.; Catlow, C. R. A.; French, S. A.; Sokol, A. A.; Bromley, S. T.; Thiel, W.; Turner, A. J.; Billeter, S.; Terstegen, F.; Thiel, S.; Kendrick, J.; Rogers, S. C.; Casci, J.; Watson, M.; King, F.; Karlsen, E.; Sjøvoll, M.; Fahmi, A.; Schafer, A.; Lennartz, C. *J. Molec. Struct. (THEOCHEM)* **2003**, *632*, 1.
- (18) Tresadern, G.; Faulder, P. F.; Gleeson, M. P.; Tai, Z.; MacKenzie, G.; Burton, N. A.; Hillier, I. H. *Theor. Chem. Acc.* **2003**, *109*, 108.
- (19) Pu, J. Z.; Gao, J. L.; Truhlar, D. G. *ChemPhysChem* **2005**, *6*, 1853.
- (20) Zhang, Y. K. *J. Chem. Phys.* **2005**, *122*, 24114.
- (21) DiLabio, G. A.; Wolkow, R. A.; Johnson, E. R. *J. Chem. Phys.* **2005**, *122*, 44708.
- (22) König, P. H.; Hoffmann, M.; Frauenheim, T.; Cui, Q. *J. Phys. Chem. B* **2005**, *109*, 9082.
- (23) Riccardi, D.; Schaefer, P.; Yang, Y.; Yu, H. B.; Ghosh, N.; Prat-Resina, X.; König, P.; Li, G. H.; Xu, D. G.; Guo, H.; Elstner, M.; Cui, Q. *J. Phys. Chem. B* **2006**, *110*, 6458.
- (24) Lin, H.; Truhlar, D. G. *Theor. Chem. Acc.* **2006**, *Online First*, DOI: 10.1007/s00214.
- (25) Day, T. J. F.; Soudackov, A. V.; Cuma, M.; Schmitt, U. W.; Voth, G. A. *J. Chem. Phys.* **2002**, *117*, 5839.
- (26) Rode, B. M.; Schwenk, C. F.; Tongraar, A. *J. Molec. Liq.* **2004**, *110*, 105.

- (27) Rode, B. M.; Schwenk, C. F.; Hofer, T. S.; Randolph, B. R. *Coord. Chem. Rev.* **2005**, *249*, 2993.
- (28) Wang, F.; Voth, G. A. *J. Chem. Phys.* **2005**, *122*, 144105.
- (29) Tongraar, A.; Kerdcharoen, T.; Hannongbua, S. *J. Phys. Chem. A* **2006**, *110*, 4924.
- (30) Rode, B. M.; Hofer, T. S. *Pure App. Chem.* **2006**, *78*, 525.
- (31) Smith, D. J.; Chandrasekhar, D.; Chaparro, S. A.; Crozier, P. A.; Drucker, J.; Floyd, M.; McCartney, M. R.; Zhang, Y. *J. Crystal Growth* **2003**, *259*, 232.
- (32) Liu, P.; Rodriguez, J. A.; Muckerman, J. T.; Hrbek, J. *Surf. Sci.* **2003**, *530*, L313.
- (33) Rega, N.; Iyengar, S. S.; Voth, G. A.; Schlegel, H. B.; Vreven, T.; Frisch, M. J. *J. Phys. Chem. B* **2004**, *108*, 4210.
- (34) Wang, J. H.; Lin, M. C. *J. Phys. Chem. B* **2006**, *110*, 2263.
- (35) Vashishta, P.; Kalia, R. K.; Nakano, A. *J. Phys. Chem. B* **2006**, *110*, 3727.
- (36) Delogu, F.; Cocco, G. *Phys. Rev. B* **2005**, *71*, 144108.
- (37) Salazar, M. R. *J. Phys. Chem. A* **2005**, *109*, 11515.
- (38) Kerdcharoen, T.; Morokuma, K. *J. Chem. Phys.* **2003**, *118*, 8856.
- (39) Kerdcharoen, T.; Morokuma, K. *Chem. Phys. Lett.* **2002**, *355*, 257.
- (40) Rode, B. M.; Hofer, T. S.; Randolph, B. R.; Schwenk, C. F.; Xenides, D.; Vchirawongkwin, V. *Theor. Chem. Acc.* **2006**, *115*, 77.
- (41) Kerdcharoen, T.; Liedl, K. R.; Rode, B. M. *Chem. Phys.* **1996**, *211*, 313.
- (42) Hofer, T. S.; Pribil, A. B.; Randolph, B. R.; Rode, B. M. *J. Am. Chem. Soc.* **2005**, *127*, 14231.

- (43) Schwenk, C. F.; Loeffler, H. H.; Rode, B. M. *J. Am. Chem. Soc.* **2003**, *125*, 1618.
- (44) Schwenk, C. F.; Loeffler, H. H.; Rode, B. M. *Chem. Phys. Lett.* **2001**, *349*, 99.
- (45) Schwenk, C. F.; Loeffler, H. H.; Rode, B. M. *J. Chem. Phys.* **2001**, *115*, 10808.
- (46) Loeffler, H. H.; Yague, J. I.; Rode, B. M. *Chem. Phys. Lett.* **2002**, *363*, 367.
- (47) Loeffler, H. H.; Rode, B. M. *J. Chem. Phys.* **2002**, *117*, 110.
- (48) Inada, Y.; Mohammed, A. M.; Loeffler, H. H.; Rode, B. M. *J. Phys. Chem. A* **2002**, *106*, 6783.
- (49) Loeffler, H. H.; Yague, J. I.; Rode, B. M. *J. Phys. Chem. A* **2002**, *106*, 9529.
- (50) Armunanto, R.; Schwenk, C. F.; Setiaji, A. H. B.; Rode, B. M. *Chem. Phys.* **2003**, *295*, 63.
- (51) Armunanto, R.; Schwenk, C. F.; Rode, B. M. *J. Phys. Chem. A* **2003**, *107*, 3132.
- (52) Schwenk, C. F.; Rode, B. M. *Phys. Chem. Chem. Phys.* **2003**, *5*, 3418.
- (53) Armunanto, R.; Schwenk, C. F.; Randolph, B. R.; Rode, B. M. *Chem. Phys.* **2004**, *305*, 135.
- (54) Armunanto, R.; Schwenk, C. F.; Randolph, B. R.; Rode, B. M. *Chem. Phys. Lett.* **2004**, *388*, 395.

- (55) Armunanto, R.; Schwenk, C. F.; Tran, H. T.; Rode, B. M. *J. Am. Chem. Soc.* **2004**, *126*, 2582.
- (56) Armunanto, R.; Schwenk, C. F.; Rode, B. M. *J. Am. Chem. Soc.* **2004**, *126*, 9934.
- (57) Schwenk, C. F.; Rode, B. M. *J. Am. Chem. Soc.* **2004**, *126*, 12786.
- (58) Hofer, T. S.; Rode, B. M. *J. Chem. Phys.* **2004**, *121*, 6406.
- (59) Hofer, T. S.; Tran, H. T.; Schwenk, C. F.; Rode, B. M. *J. Comput. Chem.* **2004**, *25*, 211.
- (60) Schwenk, C. F.; Hofer, T. S.; Rode, B. M. *J. Phys. Chem. A* **2004**, *108*, 1509.
- (61) Hofer, T. S.; Rode, B. M.; Randolph, B. R. *Chem. Phys.* **2005**, *312*, 81.
- (62) Armunanto, R.; Schwenk, C. F.; Rode, B. M. *J. Phys. Chem. A* **2005**, *109*, 4437.
- (63) Schwenk, C. F.; Hofer, T. S.; Randolph, B. R.; Rode, B. M. *Phys. Chem. Chem. Phys.* **2005**, *7*, 1669.
- (64) Hofer, T. S.; Randolph, B. R.; Rode, B. A. *Chem. Phys.* **2006**, *323*, 473.
- (65) Shah, S. A. A.; Hofer, T. S.; Fatmi, M. Q.; Randolph, B. R.; Rode, B. M. *Chem. Phys. Lett.* **2006**, *426*, 301.
- (66) Fatmi, M. Q.; Hofer, T. S.; Randolph, B. R.; Rode, B. M. *J. Phys. Chem. B* **2006**, *110*, 616.
- (67) Fatmi, M. Q.; Hofer, T. S.; Randolph, B. R.; Rode, B. M. *Phys. Chem. Chem. Phys.* **2006**, *8*, 1675.

- (68) Schwenk, C. F.; Loferer, M. J.; Rode, B. M. *Chem. Phys. Lett.* **2003**, 382, 460.
- (69) Schwenk, C. F.; Rode, B. M. *J. Chem. Phys.* **2003**, 119, 9523.
- (70) Schwenk, C. F.; Rode, B. M. *ChemPhysChem* **2004**, 5, 342.
- (71) Fatmi, M. Q.; Hofer, T. S.; Randolf, B. R.; Rode, B. M. *J. Chem. Phys.* **2005**, 123, 054514.
- (72) Hofer, T. S.; Randolf, B. R.; Rode, B. M. *Phys. Chem. Chem. Phys.* **2005**, 7, 1382.
- (73) Hofer, T. S.; Randolf, B. R.; Rode, B. M. *Chem. Phys. Lett.* **2006**, 422, 492.
- (74) D'Incal, A.; Hofer, T. S.; Randolf, B. R.; Rode, B. M. *Phys. Chem. Chem. Phys.* **2006**, 8, 2841.
- (75) Loeffler, H. H.; Mohammed, A. M.; Inada, Y.; Funahashi, S. *Chem. Phys. Lett.* **2003**, 379, 452.
- (76) Durdagi, S.; Hofer, T. S.; Randolf, B. R.; Rode, B. M. *Chem. Phys. Lett.* **2005**, 406, 20.
- (77) Xenides, D.; Randolf, B. R.; Rode, B. M. *J. Chem. Phys.* **2005**, 122, 174506.
- (78) Berendsen, H. J. C.; Postma, J. P. M.; van Gunsteren, W. F.; DiNola, A.; Haak, J. R. *J. Chem. Phys.* **1984**, 81, 3684.
- (79) San-Roman, M. L.; Carrillo-Tripp, M.; Saint-Martin, H.; Hernandez-Cobos, J.; Ortega-Blake, I. *Theor. Chem. Acc.* **2006**, 115, 177.

- (80) Loeffler, H. H.; Inada, Y.; Funahashi, S. *J. Phys. Chem. B* **2006**, *110*, 5690.
- (81) Spangberg, D.; Hermansson, K. *J. Chem. Phys.* **2003**, *119*, 7263.
- (82) Kollman, P. A.; Kuntz, I. D. *J. Am. Chem. Soc.* **1972**, *94*, 9236.
- (83) Stillinger, F. H.; Rahman, A. *J. Chem. Phys.* **1978**, *68*, 666.
- (84) Bopp, P.; Jancso, G.; Heinzinger, K. *Chem. Phys. Lett.* **1983**, *98*, 129.
- (85) Loeffler, H. H.; Rode, B. M. *J. Comput. Chem.* **2003**, *24*, 1232.
- (86) Perdew, J. P.; Ernzerhof, M.; Burke, K. *J. Chem. Phys.* **1996**, *105*, 9982.
- (87) Adamo, C.; Barone, V. *J. Chem. Phys.* **1999**, *110*, 6158.
- (88) Treutler, O.; Ahlrichs, R. *J. Chem. Phys.* **1995**, *102*, 346.
- (89) Schaefer, A.; Horn, H.; Ahlrichs, R. *J. Chem. Phys.* **1992**, *97*, 2571.
- (90) McDonald, I. R.; Singer, K. *Discuss. Faraday Soc.* **1967**, *43*, 40.
- (91) Allen, M. P.; Tildesley, D. J. *Computer simulation of liquids*; Clarendon Press: Oxford 1989.
- (92) Frenkel, D.; Smit, B. *Understanding molecular simulation: From algorithms to applications*, 2nd ed.; Academic: London, 2002.
- (93) Armin, M. v.; Ahlrichs, R. *J. Comput. Chem.* **1998**, *19*, 1746.
- (94) Li, Z. H.; Jasper, A. W.; Truhlar, D. G. *ANT; Version 2.20*; University of Minnesota: Minneapolis, 2006.
- (95) Lin, H.; Zhang, Y.; Heyden, A.; Truhlar, D. G. *QMMM; Version 1.3*; University of Minnesota: Minneapolis, 2006.

### Figure Caption

Fig. 1 Partitioning of a multilevel system into an active (core) zone, buffer zone, and environmental zone.

Fig. 2 Variation of smoothing functions  $\Phi_1$ ,  $\Phi_2$ , and  $\Phi_3$  of the sorted AP method for a system with three groups,  $i$ ,  $j$ ,  $k$ , in the buffer zone. Group  $i$  is moving through the buffer zone, group  $j$  is located at  $(r_j - r_{\min})/(r_{\max} - r_{\min}) = 0.1$ , and group  $k$  is located at  $(r_k - r_{\min})/(r_{\max} - r_{\min}) = 0.5$ . The smoothing functions  $\Phi_1$  and  $\Phi_2$  are zero when group  $i$  and  $j$  change their order;  $\Phi_2$  and  $\Phi_3$  are zero when group  $i$  and  $k$  change their order.

Fig. 3 Initial configuration for the simulation of a  $\text{Li}^+$  atom surrounded by a water cluster. The system is partitioned into an active zone with initially four water molecules, a buffer zone with initially two water molecules, and an environmental zone with initially two water molecules. The arrow illustrates the movement of the water molecule leaving the first solvation shell of the  $\text{Li}^+$  atom.

Fig. 4 Potential energy of the  $\text{Li}^+ - \text{H}_2\text{O}$  system illustrated in Figure 3 when a water molecule leaves the high-level active zone. Energies are computed with the hot spot, ONIOM-XS, permuted AP, and sorted AP methods.

Fig. 5 Magnitude of the force vector on atom H1 (see Figure 3) when a water molecule leaves the high-level active zone around a  $\text{Li}^+$  atom. Forces are computed with the hot spot, ONIOM-XS, permuted AP, and sorted AP methods.

Fig. 6 Magnitude of the force vector on the O2 and the  $\text{Li}^+$  atom (see Figure 3) when a water molecule leaves the high-level active zone around a  $\text{Li}^+$  atom. Forces are computed with the hot spot, ONIOM-XS, permuted AP, and sorted AP methods.

Fig. 7 Total energy during an MD simulation in the microcanonical ensemble. The system consists of 171 argon atoms in a periodic box with a box length of 20 Å. One atom is chosen to be the primary group, and the radius of the active zone is  $r_{\min} = 5$  Å. Trajectories are computed using the hot spot, ONIOM-XS, permuted AP, and sorted AP methods with a buffer zone 0.5 Å thick and also a scheme with an infinitesimally narrow buffer zone ( $r_{\min} = r_{\max} = 5.5$  Å). Total energy data from the simulation using the permuted AP method are directly underneath the data from the sorted AP simulation.

Fig. 8 Average temperature during an MD simulation in the microcanonical ensemble (the average is performed from the beginning of the simulation to time  $t$ ). The system consists of 171 argon atoms in a periodic box with a box length of 20 Å. One atom is chosen to be the primary group, and the radius of the active zone is  $r_{\min} = 5$  Å. Trajectories are computed using the hot spot, ONIOM-XS, permuted AP, and sorted AP methods with a buffer zone 0.5 Å thick and also a scheme with an infinitesimally narrow buffer zone ( $r_{\min} = r_{\max} = 5.5$  Å).

Fig. 9 Radial distribution function of the primary Ar atom relative to all other Ar atoms in the system. The system consists of 171 argon atoms in a periodic box with a box length of 20 Å. The radius of the active zone is  $r_{\min} = 5 \text{ Å}$ . Trajectories are computed using the hot spot, ONIOM-XS, permuted AP, and sorted AP methods with a buffer zone 0.5 Å thick and also a scheme with an infinitesimally narrow buffer zone ( $r_{\min} = r_{\max} = 5.5 \text{ Å}$ ). (a) Simulations are performed in the *NVE* ensemble. (b) Simulations are performed in the *NVT* ensemble at a temperature of 172 K.

Fig. 10 Total momentum per atom ( $\frac{1}{171} \left| \sum_{\alpha} \mathbf{P}_{\alpha} \right|$ ) during an MD simulation. The system consists of 171 argon atoms in a periodic box with a box length of 20 Å. One atom is chosen to be the primary group, and the radius of the active zone is  $r_{\min} = 5 \text{ Å}$ . Trajectories are computed using the hot spot, ONIOM-XS, permuted AP, and sorted AP methods with a buffer zone 0.5 Å thick and also a scheme with an infinitesimally narrow buffer zone ( $r_{\min} = r_{\max} = 5.5 \text{ Å}$ ). Total momentum computed in simulations using the hot spot method is illustrated on the right ordinate, whereas the scale is given on the left for the other methods. (a) Simulations are performed in the *NVE* ensemble. (b) Simulations are performed in the *NVT* ensemble at a temperature of 172 K.

Figure 1

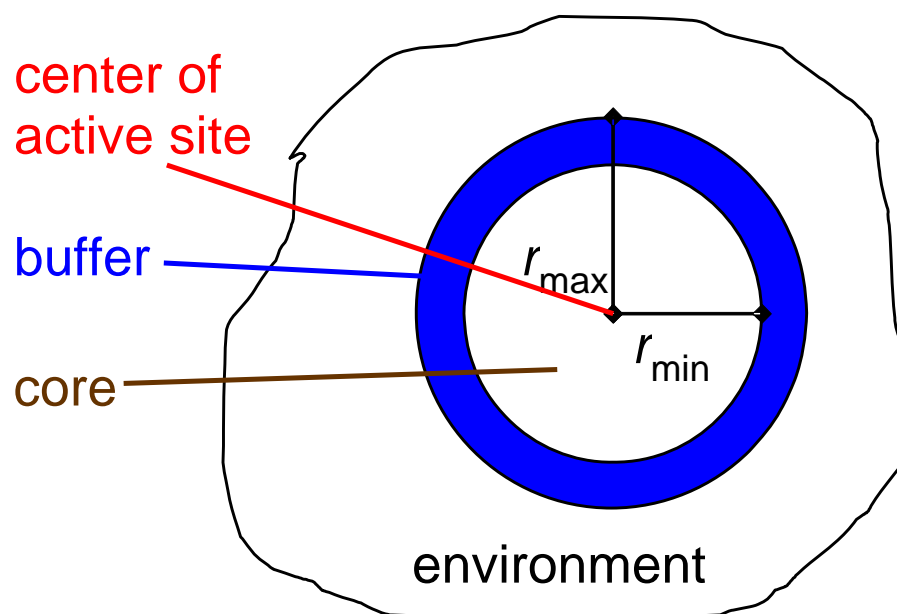


Figure 2

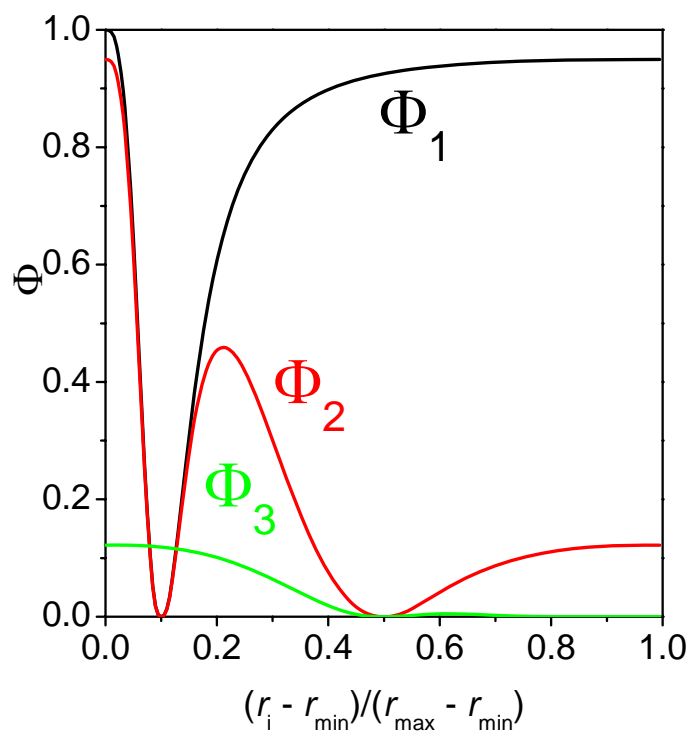


Figure 3

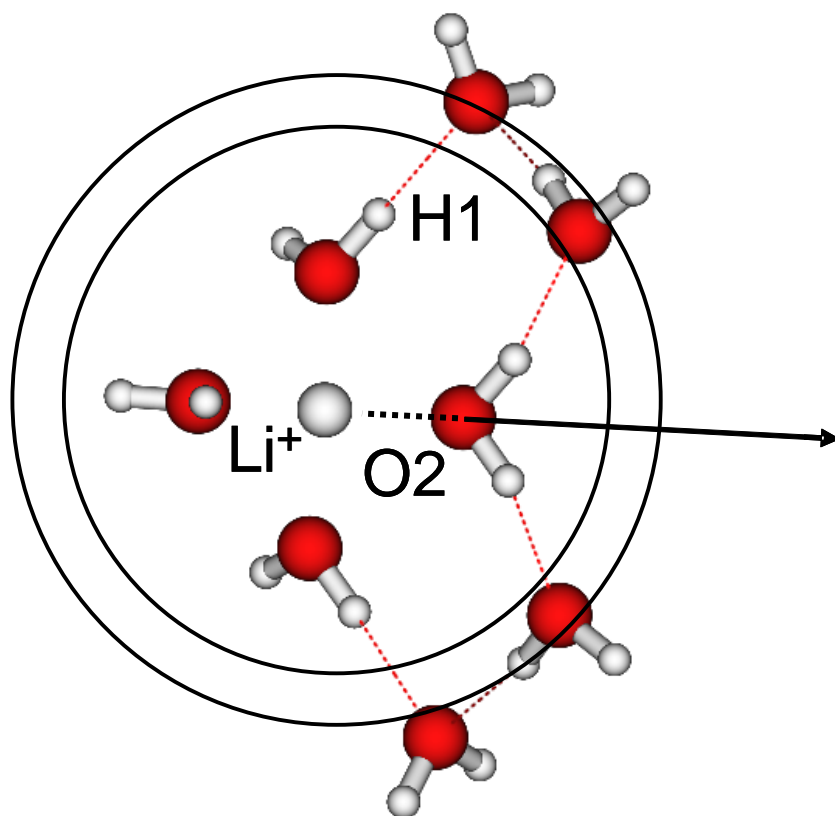


Figure 4

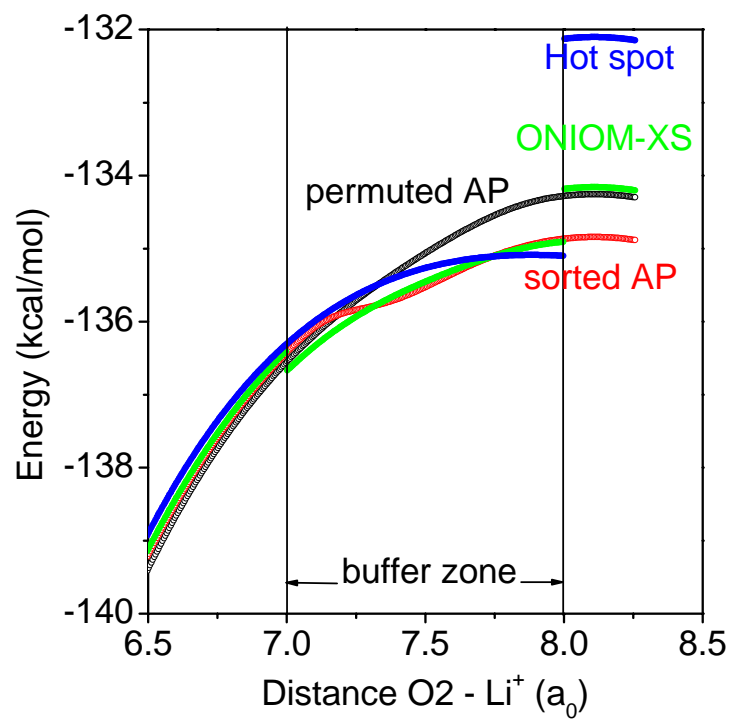


Figure 5

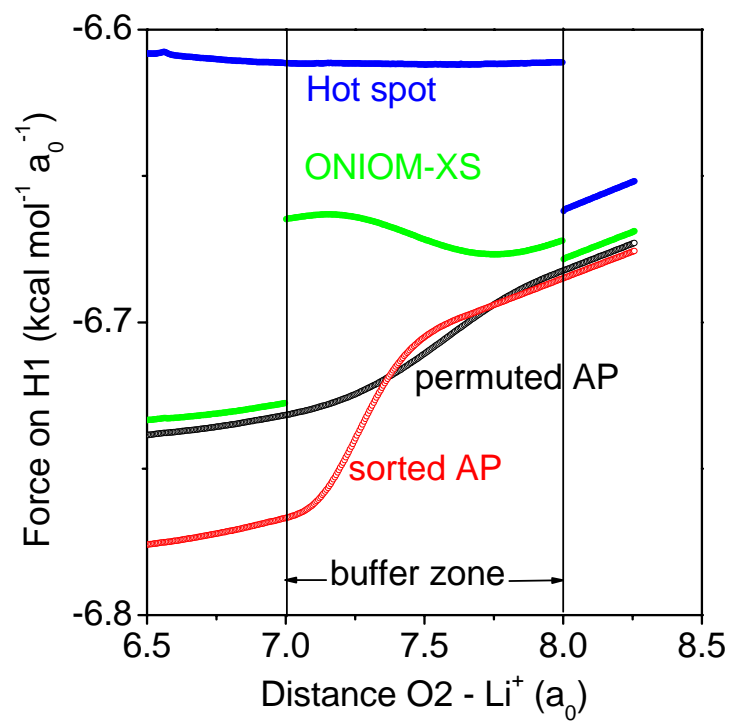


Figure 6

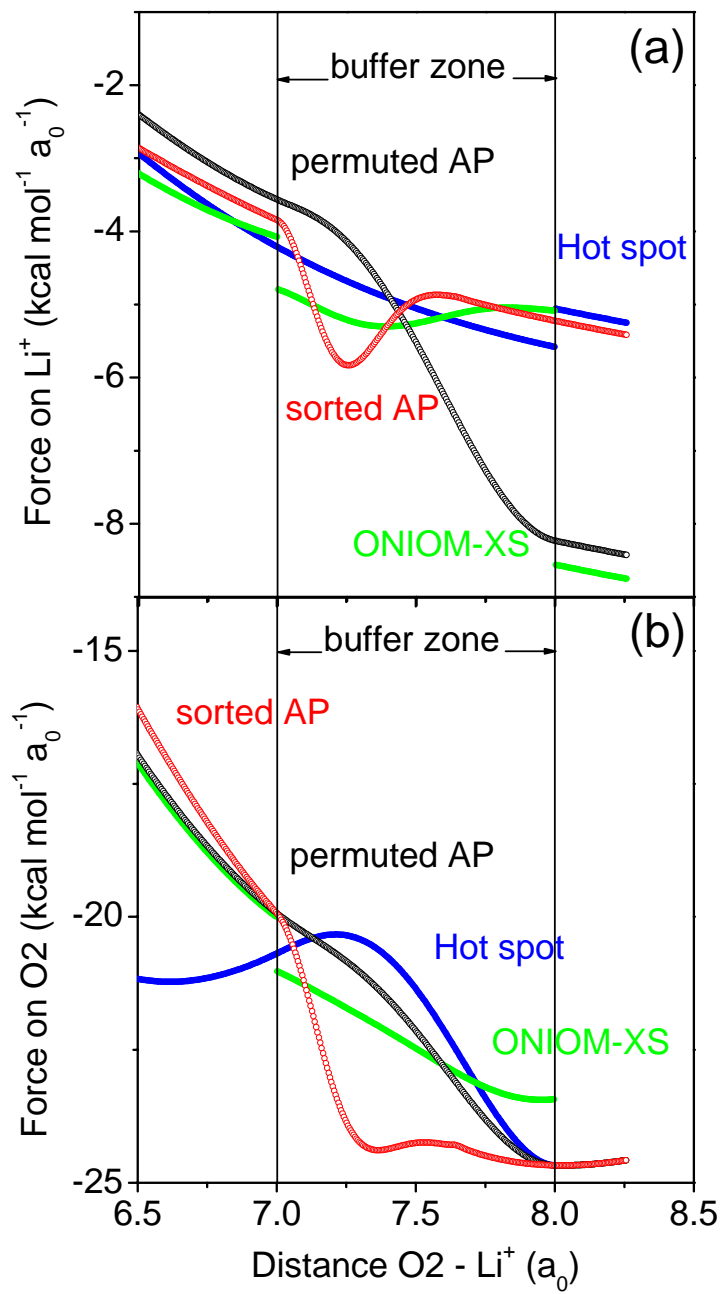


Figure 7

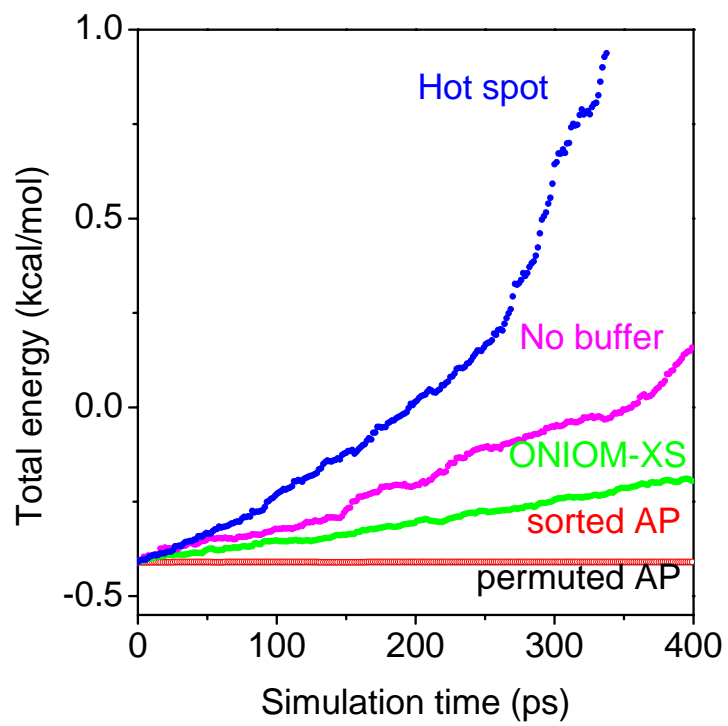


Figure 8

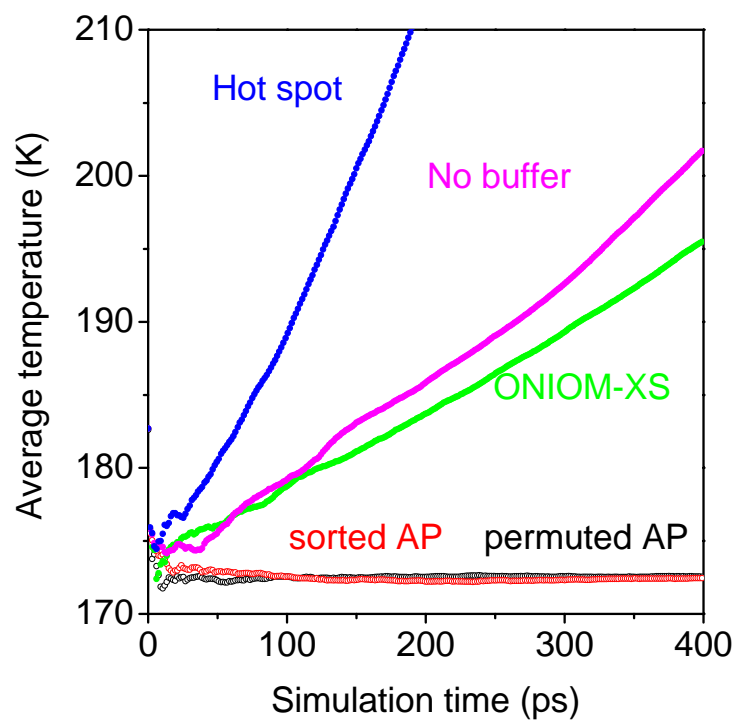


Figure 9

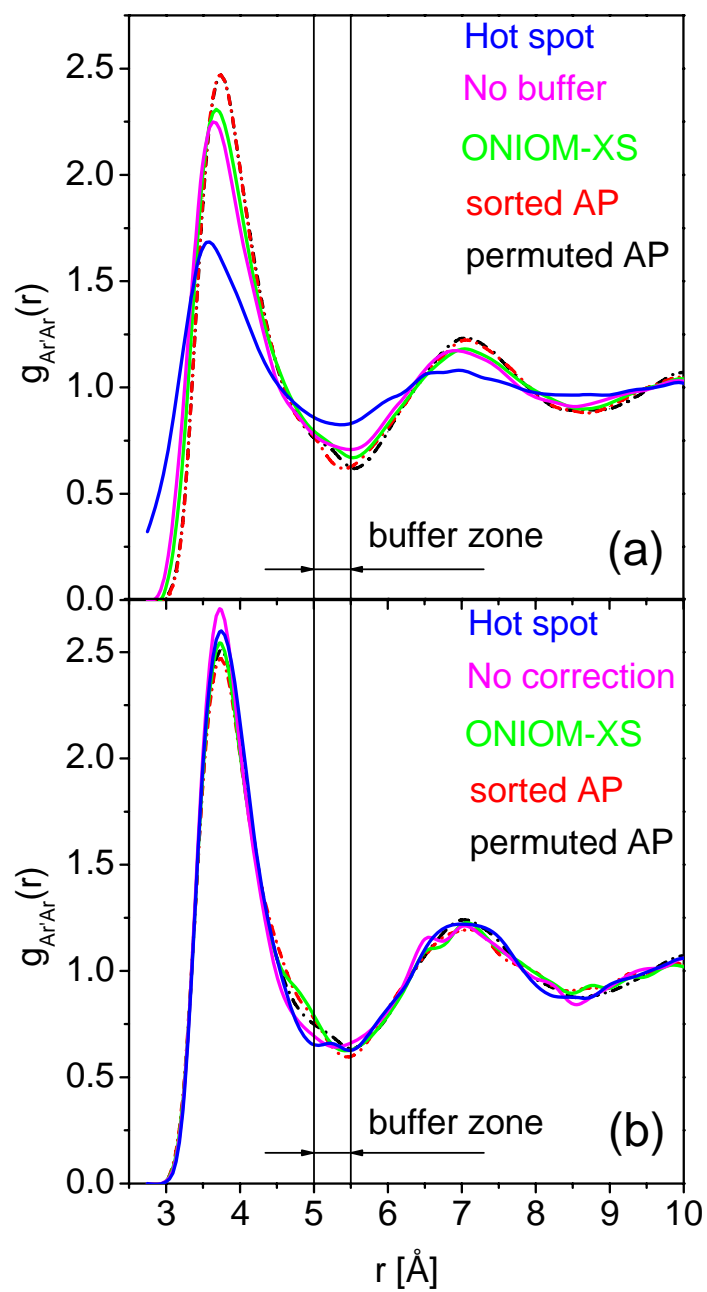


Figure 10

